A Design Optimization Strategy of an Aircraft Composite Wing-Box Based on a Multi-scale FEA

Soufiane Farah
Mechanical Structures Laboratory, Ecole Militaire Polytechnique, 16046, Algiers, Algeria.

Smail Khalfallah
Laboratory of Turbomachinery, Ecole Militaire Polytechnique, 16046, Algiers, Algeria.

Abdelwahid Boutemedjet
Laboratory of Fluid Mechanics, Ecole Militaire Polytechnique, 16046, Algiers, Algeria

Lamine Rebhi
Mechanical Structures Laboratory, Ecole Militaire Polytechnique, 16046, Algiers, Algeria.

Design optimization of composite wings is a complex problem that involves numerous material and shape parameters. This paper proposes two ideas to solve such a problem effectively, namely, the right-complex formulation of the optimization problem and the use of multi-scale finite element analysis (FEA). The first idea is achieved following a V scheme (descendant ascendant scheme). In the descent, the complexity of the problem is reduced to the lowest level (lowest-complex formulation), which may not be sufficient to get potential solutions. Accordingly, an adaptive process is performed, progressively increasing complexity by adding new variables until reaching the ***right-complex*** *formulation. The multi-scale FEA combined global and local Finite Element Method (FEM) analyses. The global one analyses the static of the global domain, which reveals the most critical panel. The latter analyses the buckling phenomenon locally and more accurately. This strategy is validated by optimizing a composite wing box from the literature and considering a well-known zone-based formulation. Therefore, the lowest-complex formulation is defined with the minimum possible number of wing zones, then adjusted by increasing iteratively the wing zone number. This process is stopped when the optimal solution becomes invariant. This application seeks to minimize the wing mass under many constraints, such as the maximum Von Mises stress. The problem is solved by coupling a Genetic Algorithm (GA) optimizer with the multi-scale FEA. Results showed that the adopted strategy detected the right-complex formulation, which significantly increased the computation time while gaining considerably in the wing mass with respect to the resistance strength criteria.*

Keywords: *Composite Wing-Box, Design Optimization, Multi-scale FEA.*

1. INTRODUCTION

In recent years, the aeronautical industry has started using composite materials, especially in some key parts of the aircraft, like the fuselage, tail, and wings [1, 2]. These materials can be designed to handle heavy loads, making them a lightweight solution that improves performance. However, optimizing how these materials are configured is challenging and often expensive due to the many factors that need to be considered along with wing design. This makes the process complex, which can lead to lower-quality solutions and high costs. Therefore, it is important to simplify these problems without losing the quality of the solution.

Composite wing box structures have been the subject of many research papers that expand from the introduction of new structural configurations and components to the optimization of the composite lay-up. These papers, such as ref [3, 4], showed clearly the high number of design parameters of a composite wing-box, which leads to highly complex optimization problems. The latter involves thousands of finite element analyses (FEA) during the optimization process. In this case, the cost of FEA has an important effect on the overall cost, which motivates the development of low-cost FE models such as the multi-scale scheme proposed in the present study. The latter may be very efficient essentially for FEA involving dynamic behavior and buckling, which is more expensive than static analysis [5-8]. Dimitrios et al. [9, 10] reported that under some conditions, multi-spar composite wing box configu–ration offers more advantages compared to the conven–tional 2-spar design. The configuration they investigated was analyzed using FEM combined with analytical formulas. In the same vein, Dähne et al. [11] and Farsadi and Dähne [12] examined the impact of variable stringer orientations on the structural response of a composite wing box besides the optimization of the laminate parameters. A multitude of research efforts have been undertaken in the field of composite optimi–zation, addressing various challenges, notably the extensive computational time required for simulations and the high-dimensional design space. Various appro–aches and techniques have been employed to tackle these issues, including the utilization of surrogate models [13, 14], parallel processing [15, 16], multi-level optimization strategies, and the reduction of design space through variable linking. In a study conducted by

Received: November 2024, Accepted: January 2025
Correspondence to: Dr Khalfallah Smail
Laboratory of Turbomachinery, Ecole Militaire Polytechnique, 16046, Algiers, Algeria
E-mail: skhalfallah16@gmail.com
doi: 10.5937/fme2501157F

Liu et al. [17], a two-level optimization strategy was implemented in conjunction with a cubic polynomial response surface to optimize a composite wing under strength and buckling constraints. In a similar work, Guo et al. [18] achieved a 34.5% weight reduction of a composite wing using a two-stage multi-objective optimization strategy. The first stage aims to optimize the laminate parameters, while the second stage focuses on aeroelastic optimization. Meanwhile, Yu Wang et al. [19] developed a three-step optimization procedure aimed at solving small optimization problems with a minimal number of design variables, simplifying the complexity of the original problem.

Some other studies combined multiple codes and software in one multi-level optimization framework to reduce the computational costs of optimization. For instance, Fischer et al. [20] optimized the layer thicknesses of a composite wing box using a multilevel optimization framework that combined a panel analysis commercial code with FE software. Likewise, Carrera et al. [21] applied a two-level optimization for the design of composite and isotropic aerospace structures with reinforced shell components. The first level consists of FEM software used to estimate the panel's loadings, while the second level code performs the optimization of the panels.

Similarly, other works [22-25] have concentrated on dividing efficient optimization procedures while considering structural and aeroelastic constraints [26, 27]. These approaches have employed various surrogate and equivalent models, including radial basis functions and equivalent plate methods, in addition to the linking of design variables, resulting in a substantial reduction in the variables set. In the same context, Jin et al. [28] used parallel GA and introduced a length indicator as a design variable to simultaneously optimize the stacking sequence and the ply thickness.

Other research papers have employed the strategy of reducing the number of design zones as a means to reduce the size of design variables. For instance, Yin Hailian et al. [29] focused on optimizing a composite wing's weight and cost by considering the layout and structural dimensions. They achieved a reduction in design variables by assuming a limited number of design zones and maintaining the same dimensions for various components within each designated zone.

Design optimization is shown to be an efficient tool to produce the best designs. It is traditionally performed in two consecutive phases: a formulation that defines the optimization problem, followed by a solving phase that produces the optimal solution for the formulated problem. The majority of the formulations are **straightforward**, which means that they transform each material and design parameter into an optimization variable. A straightforward formulation can be **over-complex** when it includes fruitless optimization variables, which leads to an extra computing cost. It can be **under-complex** when some important parameters are not included, hence producing low-quality solutions. Generally, straightforward formulations for composite structures are highly complex and likely over-complex, which raises the question of how to measure the complexity of this formulation and how to find the **right-complex** one.

Extensive studies have been recently devoted to reducing the cost of design optimization. However, the majority of them focused on the solving phase rather than the formulation one. For instance, some strategies combine global and local models [30], and others use multi-fidelity and meta-modeling-based optimization, which uses approximations for expensive solvers. These strategies are very beneficial for highly expensive solvers, but the accuracy of approximations can decrease the quality of solutions. Thus, they are not suitable for moderately expensive problems such as FEA. Accordingly, it would be efficient to improve the formulation for problems involving FEA. Indeed, an important gain can be achieved only by improving the formulation of the optimization problem. A well-known technique, which is usually used to reduce the formulation complexity, is the Analysis of Variance (ANOVA). This method has many limitations. Namely, it analyses parameters independently in the optimization context, and it may be inefficient for large-scale problems. Moreover, it is used just to decrease the number of variables. That means if the formulation is under-complex, ANOVA cannot add more variables. This motivates the proposal of a new approach to adjust the formulation as much as possible. Moreover, it must be applicable for both over and under-complex formulation. For the former, it allows for considerably reduced costs and offers the possibility of using high-fidelity solvers and adding new variables, thus improving the quality of design and reducing costs. For under-complex, it allows for further improvement of the optimal solution and gives insight into the formulation.

The present paper develops two ideas, allowing us to reduce the design optimization cost considerably. The first one is a V-approach, which defines the right-complex formulation of a design optimization problem starting from a straightforward formulation, which is considered here as an input for the proposed V-approach. This means that the V-approach represents a step that can be applied after the formulation of the optimization problem. It is achieved via a V scheme (descendant ascendant scheme). The descendant scheme is applied to an input formulation, which is generally straightforward, giving the lowest-complex formulation. Then, an adaptive process that increases progressively the complexity of the latter until reaching the right one to get the global solution. Therefore, this iterative process must start with the lowest possible number of decision variables, which should explore the design space. Then, in each iteration, the optimization problem is solved, and its formulation is evaluated by comparing the current solution with the previous one. If this comparison shows that the formulation can be improved, new decision variables are added to a zone that ensures a balance of exploration/exploitation. This method is applied to a wing-box prototype from the literature. The results show that the complexity is reduced considerably while the solution is not altered.

The second idea is applied when solving the formulated problem in order to reduce further the cost. It is a multi-scale FEM analysis, which performs a static FEA on the global domain, allowing to select the most critical zone. The latter is analyzed considering buckling using a local FEA.

The remaining parts of this paper present, firstly, the prototype selected as an illustrative example during the description of the method. Then, a motivation section will be presented, which will show the difficulty encountered with composite materials optimization, fol–lowed by a description of the key mechanisms of the proposed method. The last section presents the out–comes of the application of the proposed method on the selected prototype.

2. ILLUSTRATIVE CASE STUDY

An illustrative application is presented in the description section to describe the proposed method's key mecha–nisms better. This application is performed considering a prototype from the open literature. This application allows us to expose the method's key features and validate its efficiency via the outcomes.

The wing-box prototype studied in this work is the semi-monocoque structure used by Benaouali et al. [31]. Table 1 gives the main features and parameters of the external geometry of this prototype.

Table 1. Parameters of the wing planform

Parameter	Value
Aspect ratio (-)	9.4
Taper ratio (-)	0.3
Leading edge sweep angle (deg)	27.5
Semi span b/2 (m)	16.96
Root chord (m)	7.01
Trapezoidal chord ratio (-)	0.71
Kink position ratio (-)	0.37
Root-kink-tip twist angles (deg)	0

As shown in Fig. 1, the considered wing-box struc–tural layout is made up of a set of skin panels, 2 spars, 27 ribs, and 16 skin stiffeners for each of the upper and lower skin panels, besides 4 spar caps attached to the spar's webs. The two spars consisting of the front and rear spars follow the leading and trailing edges shapes and are located at 15% and 75% of the airfoil chord, respectively. On the other side, the wing-box ribs are positioned at uniform distances along the wing span and are parallel to the flight direction. The skin stiffeners or stringers are also, in turn, distributed equidistantly on the upper and lower skin surfaces between the front and rear spars.

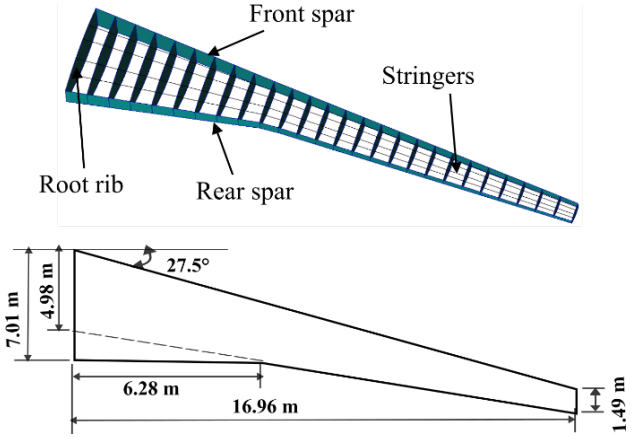

Figure 1. An overview of the considered wing-box structural components

In the original work of Benaouali et al. [31], the entire wing -box is made of the isotropic 2024-T351 aluminum alloy. In the present study, except for stringers and spar caps, which are made of the isotropic 2024-T351 aluminum alloy, all the remaining structural components are made of composite unidirectional carbon fibers/epoxy. Table 2 lists the properties of the relevant material.

Among the various composite materials, carbon and glass fiber composites are the two most commonly used in the aerospace industry. As noted in reference [32], several airliners, including the Boeing 757, 767, and 777, as well as the Airbus A310, A320, A330, and A340 from Europe, feature numerous structural components made from these materials. However, carbon fibers are preferred over glass fibers, particularly in major struc–tural components like wings and tails, due to their supe–rior specific modulus and specific strength, as high–lighted in reference [33]. Additionally, carbon fibers offer a better overall balance of properties, such as an improved weight-to-strength ratio, the ability to form complex shapes, reduced material waste, enhanced fati–gue resistance, and superior corrosion resistance. For these reasons, carbon fiber composite material was se–lected for this study, in addition to its excellent property balance and its established history of use in the aerospace industry.

Table 2 Materials properties [31, 34]

Carbon/Epoxy UD300	
Property	Value
Young's modulus E_{11} (Mpa)	119.3e3
Young's modulus E_{22} (Mpa)	8.2e3
Shear modulus G_{12} (Mpa)	3.6e3
Poisson's ratio ν12	0.34
Longitudinal tensile strength X^t (Mpa)	2282
Longitudinal compressive strength (MPa)	1067
Transverse tensile strength (MPa)	54
Transverse compressive strength (MPa)	200
Shear strength S (Mpa)	99
2024-T351 aluminum alloy	
Property	Value
Young's modulus E (Mpa)	73.1e3
Yield strength σ_{yield} (Mpa)	324
Ultimate strength σ_u (Mpa)	469
Poisson's ratio ν	0.3
Density ρ (kg/m^3)	2.78e3
Allowable stress σ_{allow}	1.5 x σ_{yield}

3. MOTIVATION

The formulation of an optimization problem refers to the definition of the objectives, the constraints, and the decision variables as mathematical formulas. In fact, a problem can be formulated in different manners. For instance, in the present study, we aim to reduce the wing-box mass while keeping it resistant under different structural solicitations. The decision variables adopted in this work are related to the wing-box structure's material properties.

The difficulty of using composite materials compa–red with isotropic ones is in modeling the reduction of the different component thicknesses along the wing span-wise. This can be handled via three manners: a) by

changing the number of plies while keeping their thickness constant, ii) by changing the thickness of each ply and keeping the number constant, iii) by changing both the number of plies and their thickness (the work of [35] for instance). The third variant is the most complex, while the first and the second variants can produce the required representations, as can the third one. The first variant is more practical since changing the number of plies is easier than changing their thickness, as used in reference [36].

On the other hand, these composite material properties must change from one design zone to another, which are shown in Fig. 2. This figure shows that the number of design zones is very important. Indeed, between every two ribs, there are five design zones (zone of upper skin, lower skin, two spars, and the rib). This makes a total number of 26 times 5 design zones. This consideration is because, from one zone to another, the structural loads may change. Subsequently, the thickness of all components (panels, spars, ribs) must be more important near the root than near the tip of the wing. Accordingly, each zone must be assigned its own material properties. However, this manner of modeling may increase drastically the number of optimization variables. For instance, in the present study, if the number of plies changes in each zone, it results in a number of variables of 26 times the considered material properties. If the number and the orientation of plies are considered as optimization parameters, it gives at least a total number of (26 x 2 x 5) optimization variables. This number of variables is very important since the objectives are evaluated using FEM solvers. Yet, this number seems exaggerated, and it may exist in two adjacent zones with negligible differences and can be assigned with the same variable values. This raises the question of how to find the minimum sufficient set of optimization variables. In order to answer this question, the adaptive process shown in Fig. 3 is proposed.

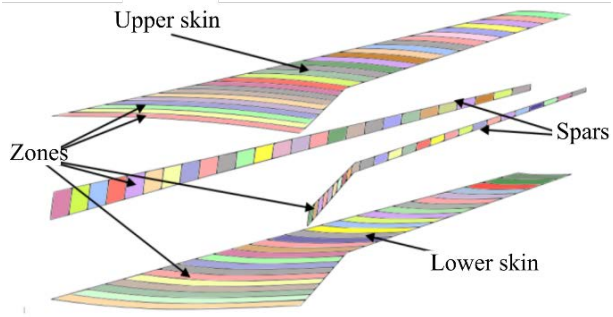

Figure 2. Optimization design zones [31]

4. DESCRIPTION OF THE PROPOSED V-APPROACH

Figure 3 illustrates the flowchart of the proposed V-approach. Its input is called the *initial formulation*, which can be straightforward. As mentioned above, this initial formulation may be over-complex for composite design optimization.

Based on this initial formulation, the number of variables is reduced as possible, giving the lowest-complex formulation. The mechanism of how to construct it is explained below (section 4.2).

As shown in Fig. 3, the V-approach is an iterative process. In each iteration, the formulation is modified by adding new variables. The new problem is then solved, and its optimal solution is compared with the previous iteration. This process is stopped when reaching an invariant solution. This produces an optimization problem with the right complexity.

Solving this problem requires a selection of an optimization technique, a FEM solver, and an automatic coupling between them, as explained below in section 4.3.

In order to validate this process, it was applied to the illustrative case study (section 2).

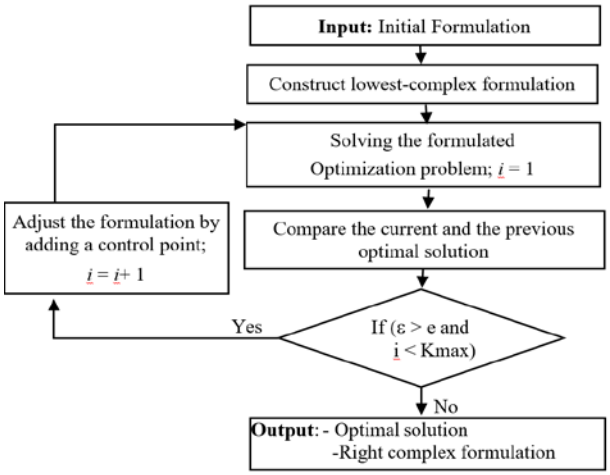

Figure 3. Flowchart of the proposed method

4.1 Initial formulation

In the present study, the zone-based formulation is adopted to generate an initial formulation (input). This type of formulation was selected since it is well-documented and widely used, which allows for efficient testing of the proposed V-approach. This formulation is based on dividing the wing into a set of zones, on each of which a set of decision variables is defined. This formulation is used by Seresta et al. [37], who divided the wing skin into 9 panels and considered the composite properties on each panel as decision variables. Zhang et al. [38] have divided the wing into 29 areas in total, including all the components of the wing. Kilimtzidis et al. [39] have also considered decision variables on 06 zones of the wing. In these studies, the effect of the number of zones was not investigated. Thus, it can be over-estimated, which leads to an extra computing cost, or under-estimated, leading to a lower quality of solutions. The complexity of this formulation is adjusted in the present work using the proposed V-approach, which allows the selection of the right number and location of the wing zones.

4.1.1 Design variables

A straightforward formulation of this problem is to consider the number of plies and their orientations on each zone of the wing as decision variables, as well as the shape of the wig. However, this has led to an extremely complex problem. Validating the proposed approach to a problem limits the number of tests, which prevents investigating the different situations of

operation and the applicability, such as the effect of the refinement strategy. Therefore, in order to allow more comparisons of these strategies, the initial formulation does not consider all the previous aspects. Instead, it considers only the plies number as a variable without changing their orientations and the layout shape. At the same time, adequate orientations are obtained from the literature. Indeed, considering the orientations of the fibers increases the complexity considerably and reduces the number of tests. At the same time, the primary goal of the present work is to perform the maximum of tests of the proposed strategy instead of focusing on one application.

In order to select the adequate orientation, many researchers, such as [40] and [41], performed optimization of ply orientation for wing boxes. The findings of Aung et al. [40] are considered in the present work. Figure 4 presents the adopted orientations. These orientations are in agreement with the physical beha–vior. Indeed, 0° orientation is adequate for spars and skins in order to support bending, whereas ±45° is ade–quate for ribs, which must support torsional loads [40].

On the other hand, in order to guarantee symmetry and balance, the wing box is built by superposing a sequence of ply groups instead of plies (Fig. 4). Each ply group is composed of a set of plies, which ensures symmetry and balance. The skins and the spars ply-group consist of 02 adjacent 0° plies. Whereas a rib ply-group consists of 06 plies (45°/-45°/0°/0°/-45°/45°) (Fig. 4). In order to maintain this symmetry, it is nece–ssary to consider the ply-group number as a decision variable instead of the ply number.

Finally, the initial formulation is to find the optimal ply-group number for 05 components (2 skins, 2 spars, and 01 rib) for each zone. This is still an over-complex problem. Indeed, among the total design variables zones (26), it may exist adjacent zones with the same pro–perties. Accordingly, a control point (CP) based method is adopted, as shown in Fig. 5. The principle of this method is to impose the ply-group number on some lo–cations, which are called control points (CPs). Whereas the remaining zones have numbers of ply groups obtained from a linear interpolation between the two adjacent control points. This linear function can be justified by the distribution of aerodynamic loads that also follow a decreasing curve. In the following equations, *mbr* refers to the structural members of the wing box such as the ribs, lower/upper skins, and front/rear spars; $Np_j^{mbr}(y)$ is the number of ply-group of the structural member (*mbr*) at a design zone (j), which is located at a position *y* of the span direction. Np_j^{mbr} Can be easily determined as a function of the ply-group number $\left(Np_{cp\_i}^{mbr}\right)$ and $\left(Np_{cp\_i-1}^{mbr}\right)$ of its adjacent control points (CP_i and CP_i-1) as given in equation 1:

$$Np_j^{mbr}(y)=\left(\frac{Np_{cp\_i-1}^{mbr}-Np_{cp\_i}^{mbr}}{y_{cp\_i-1}-y_{cp\_i}}\times y+Np_{cp\_i-1}^{mbr}\right), \quad (1)$$

$$with\ y\in\left[y_{cp\_i-1},y_{cp\_i}\right] \qquad (01)$$

where y_{cp_i-1} and y_{cp_i} are the coordinates of the adjacent CPs, while $Np_{cp\_i-1}^{mbr}$ and $Np_{cp\_i}^{mbr}$ repre–sents the laminate ply-group numbers at the adjacent CPs of the structural member *mbr*.

In this way, the initial design vector includes, for each control point *i*, five design variables: $Np_{cp\_i}^{upper\ skin}$, $Np_{cp\_i}^{lower\ skin}$, $Np_{cp\_i}^{rear\ spar}$, $Np_{cp\_i}^{front\ spar}$ and $Np_{cp\_i}^{rib}$. Therefore, the initial vector of decision variables *X contains 5. N* variables. Where *N* is the numbre of control points.

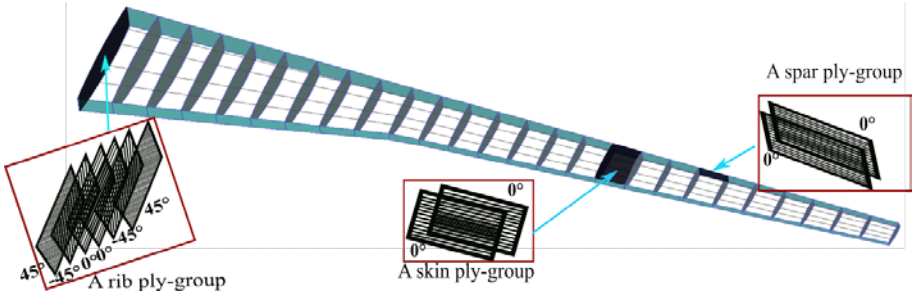

Figure 4. Adopted ply orientation for the different parts of a wing box.

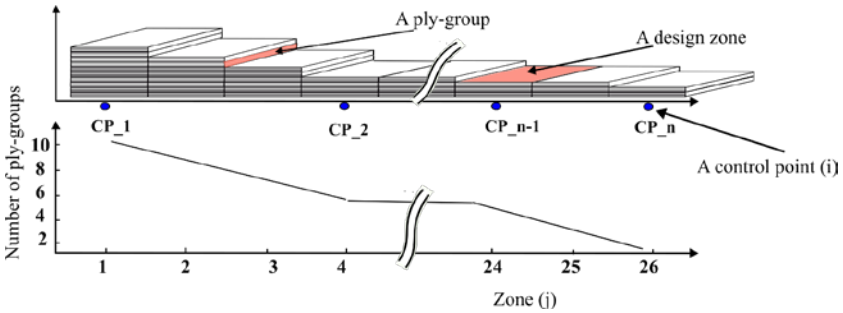

Figure 5. Adopted control points-based method for ply number generation of the different zones of the skin.

4.1.2 Objective function and constraints

The goal of this optimization process is to minimize the overall wing-box mass while meeting the various structural requirements, such as maintaining strength and controlling displacement and twisting at the wing tip. The objective function can be formulated as the sum of weights of all the wing-box structural components, which depends on the design vector $\boldsymbol{X}$ and the total number of elements constituting the wing-box finite elements model (FEM):

$$f_{obj}(X) = \sum_{j=1}^{5\times 26} W_j(X) \tag{2}$$

where W_j is the weight of the j-th element of the wing-box, which are the 5 elements (rib, lower/upper skins, and front/rear spars) at the 26 zones. This objective function is minimized with respect to a given set of constraints related to the structural requirements. The first constraint corresponding to the material failure is formulated by the mean of Tsai-Wu and Von Mises failure criteria depending on the structural component material (composite or isotropic) [30]:

$$\begin{aligned} C1: &\frac{\sigma_x^2}{X^t X^c} + \frac{\sigma_y^2}{Y^t Y^c} - \sqrt{\frac{1}{X^t X^c}\cdot\frac{1}{Y^t Y^c}}\sigma_x\sigma y + \\ &\left(\frac{1}{X^t} - \frac{1}{X^c}\right)\sigma_x + \left(\frac{1}{Y^t} - \frac{1}{Y^c}\right)\sigma_y + \frac{\tau_{xy}^2}{S^2} - 1 \le 0 \end{aligned} \tag{3}$$

$$C2: \frac{\sigma_{VM}}{\sigma_{allow}} - 1 \le 0 \tag{4}$$

where σ_x, σ_y, and τ_{xy} represents the ply stresses expressed in the ply coordinate system and σ_{VM} is the Von Mises equivalent stress, while X^t, X^c, Y^t, Y^c, and S are the allowable stresses of the ply and σ_{allow} is the allowable stress of the isotropic material (Table 2). On the other hand, the vertical displacement d_{tip} and torsional twist θ_{tip} at the wing tip must stay under certain reference values [30]:

$$C3: \frac{d_{tip}}{d_{ref}} - 1 \le 0 \tag{5}$$

And

$$C4: \frac{\theta_{tip}}{\theta_{ref}} - 1 \le 0 \tag{6}$$

The same values used in the work of Panettieri et al. [30], $d_{ref} = 0.2 \times b/2$ and $\theta_{ref} = 6°$ are adopted in the present study. A last optimization constraint is set to prevent buckling of the most critical stiffened panel in the upper and lower skins; this is achieved by ensuring that the buckling factor of the panel is bigger than a safety factor set equal to 1.5 in this study:

$$C5: 1.5 - \lambda_{cr} \le 0 \tag{7}$$

Calculation of constraint C5 requires two steps: selection of the critical stiffened panel and construction of a local finite element model (LFEM) for buckling analysis. More details are provided in the next sections. In summary, the formulated optimization problem is given as follows:

$$\begin{cases} \min f_{obj}(X) \\ subject\,to \\ X_L \le X \le X_U \\ C1 \le 0 \\ C2 \le 0 \\ C3 \le 0 \\ C4 \le 0 \\ C5 \le 0 \\ Tip\,thickness \le Root\,thickness \end{cases} \tag{8}$$

The formulated problem without the last constraint is sufficient to obtain a physically accepted solution. However, it may require a huge number of computations. In order to reduce the solving cost further, an additional constraint on the thickness of the wing is added. This constraint represents the physical behavior of the wing in that the near root region is thicker than the near tip. This last constraint on the thickness allows faster convergence since the configurations with thicker tips are not solved by the FEM solver.

4.2 Construction of the lowest-complex formulation

As mentioned previously, the proposed V-approach has to be applied to an existing initial formulation for which the set of decision variables has already been defined. Accordingly, the reduction of this set is achieved by suppressing the maximum number of decision variables.

However, this operation can be performed in different ways and may lead to different formulations, which raises the question of how to construct an efficient lowest formulation. The answer to this question is based on the fact that an efficient formulation must explore the maximum of the design space. A well-explored design space allows the discovery of the best designs and allows adding efficiently new decision variables during the adjustment process in the proposed procedure (Fig. 3). Many methods and criteria are proposed in the literature to ensure exploration, such as the Latin Hyper Cube method and the MaxMin distance criterion [41]. The selection of a criterion depends on the type of problem. Moreover, the suppression of initial variables must not exclude variables necessary for the main characteristics of the problem.

For instance, for the tested illustrative example, the maximum distance criterion is suitable. This means that the distance between CPs must be the maximum possible distance. On the other hand, the adopted method to generate a wing-box design is based on the interpolation of the composite properties between control points. Accordingly, the lower possible number of CPs to perform an interpolation is 2. Moreover, the distance between these 2 CPs must be the maximum. This leads to the 2 CPs located on the ends of the wing (tip and root) (CP_1 and CP_n in Fig 5).

As a result, the initial design vector includes 10 variables: 04 ($Np_{cp\_1}^{upper\,skin}$, $Np_{cp\_2}^{upper\,skin}$,

$Np_{cp\_1}^{lower\ skin}$, $Np_{cp\_2}^{lower\ skin}$) for the lower and upper skins, 04 ($Np_{cp\_1}^{rear\ spar}$, $Np_{cp\_1}^{front\ spar}$, $Np_{cp\_2}^{rear\ spar}$, $Np_{cp\_2}^{front\ spar}$) corresponding to the rear and front spars elements, and 02 related to the ribs $Np_{cp\_1}^{rib}$ and $Np_{cp\_2}^{rib}$.

$$X = \left\{ \begin{array}{l} Np_{cp\_1}^{upper\ skin}, Np_{cp\_2}^{upper\ skin}, p_{cp\_1}^{lower\ skin}, Np_{cp\_2}^{lower\ skin}, \\ Np_{cp\_1}^{rear\ spar}, Np_{cp\_2}^{rear\ spar}, Np_{cp\_1}^{front\ spar}, Np_{cp\_2}^{front\ spar}, \\ p_{cp\_1}^{rib}, Np_{cp\_2}^{rib} \end{array} \right\}$$

4.3 Solving the formulated optimization problem

Solving the above-formulated optimization problem requires the coupling of a FEM solver and an optimi–zation algorithm into one framework, where the com–munication between the different parts must be automated.

4.3.1 Description of the Adopted Optimization Technique

Genetic algorithms (GA) are one of the most used techniques in the optimization of ply-number in composite wings. Many researchers reported that GA is well adapted to discreet problems [37, 42, 44, and 45]. It is also suitable for problems with local optima owing to its stochastic character. As shown in Fig. 6, GA is a population-based method; it starts with a random population, which is then moved iteratively toward the optimal solution. The principle of moving the population is based on a natural selection mechanism, similar to a biological evolution. Each individual in the population is evaluated in terms of objectives and constraints using a FEM solver. This operation is performed in parallel by dividing the population into many subpopulations. Genetic operations perform a selection of parents and generate offspring via cross-over and mutation. This produces a population of children that merges with the parents in order to guarantee elitism. Then, a population of *P* individuals is selected from the merged population.

The two main parameters controlling the solution quality are the population size *P* and the number of generations (iterations). In order to ensure that the obtained solution is independent of these parameters, many tests were performed. The number of iterations is selected by observing the iterative process. In conclusion, all the tested configurations converged at about 50 generations. Many population sizes were tested, starting from a population size of 150, which required about 70 hours for each optimization using parallel computing on stations of 64 G of RAM and 24 Xeon processors of 2.4 GH. The number of performed optimizations to reach the right-complex formulation is around 5 (5 CPS) for each strategy. The performed tests reveal that the population size (150) is weak, especially when increasing the number of control points (CP). Indeed, this population size corresponds to 15 times the number of variables for 2 CPs and only 06 times the number of variables for 5 CPs (each CP corresponds to 5 optimization variables). For this reason, the population size was increased to reach a population size where the solution for 5 CPs is invariant, which is 200.

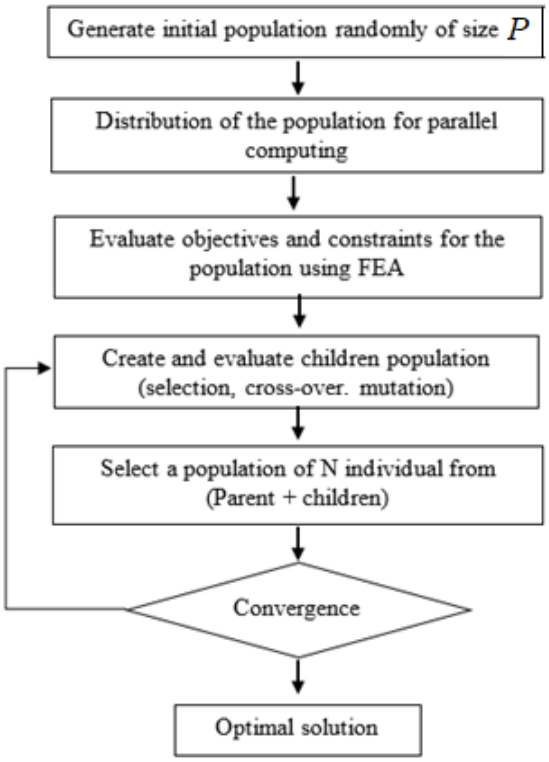

Figure 6. Schematic of the adopted GA algorithm.

4.3.2 Finite Element Analysis

The structural response of the wing-box components is assessed through a finite element model using ANSYS APDL FE commercial software. The adopted model makes use of different element types depending on the loads carried by the concerned component in order to reduce the global number of degrees of freedom (DOFs). As a result, the thin-walled structures such as the skin, spar webs, and ribs are modeled as shell elements (SHELL181) with 6 DOFs per node, while the spar caps and stringers are idealized as rod elements that work on traction and compression only (LINK180) with 3 DOFs per node. When necessary, the connection between the different elements is ensured through node merging. Regarding the mesh topology, all surface elements are generated using quadrilateral and triangular elements with 4 and 3 nodes, respectively, depending on the regularity of the surface (Fig. 7.b).

As a way to eliminate the effects of elements size on the FEM results, a mesh convergence study has been conducted to determine an optimal mesh size. Since the outer and internal geometries of the wing are not included in the design variables, this optimal mesh is generated only one time and used for all the FE simulations.

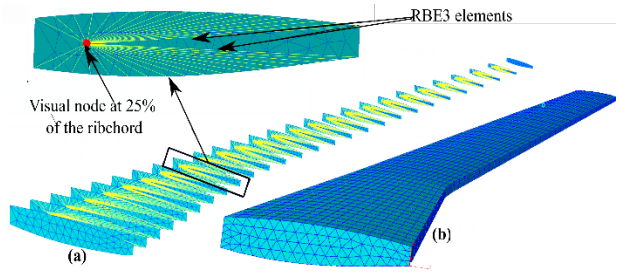

Figure 7. a. Application of lift force at ribs b. Wing-box finite element mesh example

As shown in Fig. 8, the three critical and inde–pendent criteria used in optimization as constraints and evaluated by FEA are considered to check the mesh convergence. Therefore, ten (10) meshes were generated and used in FEA, giving the failure index and disp–lacement distributions presented in Fig. 8. As observed, starting from the mesh 73000 elements, the variation of the selected criteria becomes negligible with respect to the mesh size, especially for the Tsai-Wu criterion. The mesh of 88000 elements was selected for the present optimization. The maximum difference between the criteria values of the selected mesh and the most refined one (170000 elements) is the 2.3% Von-Mises criterion.

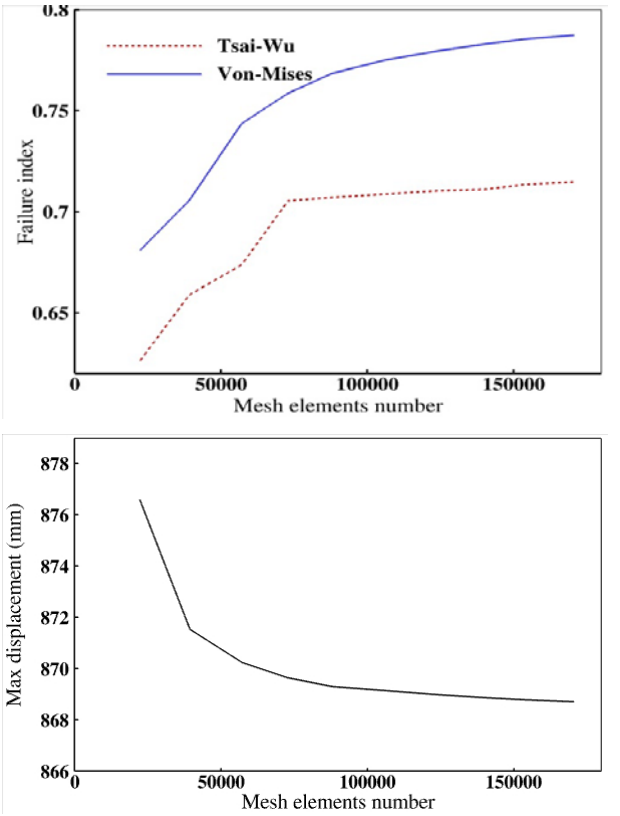

Figure 8. Results of the mesh convergence study

Regarding the boundary conditions, a load is applied on the wing, as shown in Fig. 9. The value of this load is obtained from the references [30 and 31]. It is a symmetric pull-up maneuver at diving speed V_D = *200 m/s*, considering a vertical load factor n = 2.5. The estimation of the aerodynamic loads acting on the wing is achieved by calculating the total lift using the average cruise lift coefficient of the wing C_L = *0.58* [31]. The resultant force L_T is calculated by the mean of equation 9. Then, it is applied on a spanwise line of the wing located at 25% of the airfoil chords (Fig. 9) [7]. This load is spread out considering an elliptical distribution along the application line, as shown in Fig. 9.

$$L_T = \frac{1}{2} n \cdot C_L \cdot \rho \cdot V_D^2 \cdot S \tag{9}$$

where ρ and S are the air density and the wing surface, respectively. The load is applied through the establis–hment of a virtual node at this specific location, which is subsequently connected to the boundary nodes of the respective rib using RBE3 elements (Fig. 7.a). On the other hand, the wing-box root section is fixed by setting all the DOFs to zero.

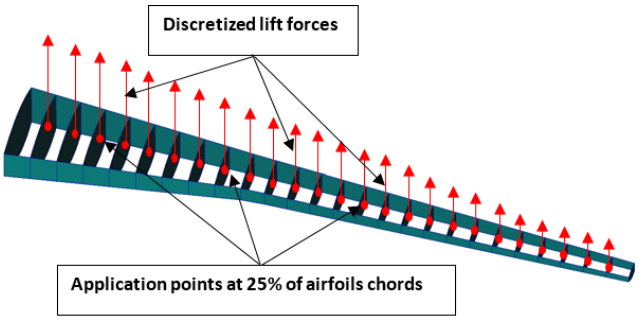

Figure 9. Load applied on the FEM model

The aforementioned model can be seen as a global finite element model (GFEM), and it is used to calculate the constraints C1, C2, C3, and C4 , while the constraint C5 is verified by the mean of a local (LFEM) that is constructed based on the results of the GFEM. The panel subjected to the maximum stringers' compressive loads is then considered critical. Once the critical stiffened panel is selected, a detailed FEM is built using the loads and geometry from the GFEM. Precisely, the stringers are no longer rod elements and are now replaced by shell elements, forming a T cross-section while preserving the same area of 375 mm^2 . A buckling analysis is performed on the LFEM to determine the critical factor of this panel.

4.3.3 Coupling of the FEM solver and GA

The coupling of the FEM (GFEM and LFEM) and the optimization algorithm is achieved by adopting a batch mode running of the implemented programs. The GA optimizer is the pilot, which generates a population in each generation. For every individual of the population, which represents a wing-box prototype, a command line instruction is launched in the FEM solver to evaluate the different constraints (C1, C2, C3, C4, and C5) and the objective function. The FEM program is launched using a pre-established MACRO, allowing it to generate mesh, run computations, and export results for a given optimization variable vector X.

4.4 Convergence criterion

The role of the iterative process shown in Fig. 3 is to construct the efficient set of decision variables that produce the optimal solution. After adding a CP, the formulation is enriched with new variables, which requires solving the problem again, which may produce

a better optimal solution. Nevertheless, it must be stopped when the added optimization variables do not produce a significant improvement in the objective function. This criterion (ε) is a measure of the relative difference between the objective function value of the current and the previous iteration (ε = (Solp – Solc)/ Solc). Where Solp is the optimal mass before adding a CP, Solc is the optimal mass after adding the current CP. The limit value of ε at which the process is stopped (e) is a user-defined parameter.

4.5 Adjusting the formulation of the optimization problem

In the case when convergence has not been reached, the current formulation can be improved by adding new decision variables, which creates a new formulation of the optimization problem. The latter should be solved again, which constructs the iterative process. This process of adding new decision variables, which is called refinement here, depends on the over-complex formulation (the input), similar to the generation of the lowest-complex formulation. The refinement consists of inserting new variables gradually until the solution becomes invariant. In the same way as the initial generation of formulation, the refinement process is not unique, and the quality of the final formulation depends on the criterion used to select the added variable. Accordingly, adding new design variables must guarantee two conditions: the exploration of the remaining design space and the exploitation of the sampled space. The exploitation means that the added decision variables must produce an improvement of the optimal solution. Indeed, after adding variables, the problem is solved again in each iteration, and the solution is compared with the previous one.

For instance, in the treated example, the initial formulation is constructed by considering only the two edge zones of the wing. Then, new zones (or CPs) are added iteratively during the refinement process until convergence (Fig. 10). In order to show the effect of the refinement criterion; three strategies are tested, as presented in section 5 (refinement strategy 1, 2, 3).

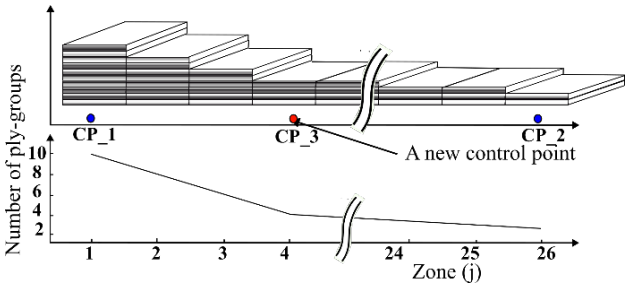

Figure 10. Adjusted formulation with three control points

5. RESULTS AND DISCUSSION

This section presents an application of the proposed method on a prototype from the literature, which is the illustrative case study presented in section 2. Therefore, the proposed approach is implemented as explained in the previous section. The lowest-complex formulation is based on two control points (CP_1 and CP_2) selected initially at the ends of the wing, which gives initially 10 decision variables. As mentioned before, the criteria for selecting the refinement CP may have an effect on the cost and the results of this approach. Therefore, in the present work, three refinement strategies to add new control points are tested:

- **Refinement strategy 1:** This strategy is called uniform refinement. The principle of this strategy is that all the control points in a given iteration must be distributed uniformly along the span wise direction. This means that the control points change their positions from one iteration to another.
- **Refinement strategy 2:** This strategy is called hierarchical refinement. This is in contrast to the previous strategy, in which changing the position of the control points from one iteration to another may not be efficient. This strategy does not change control points from one iteration to another. Thus, a new point is added between exiting control points.
- **Refinement strategy 3:** This is an adaptive strategy, as shown in Fig. 11. The main idea of this strategy is to exploit the constraints results from the FEA of the current iteration in order to efficiently choose the next CP. Indeed, adding a new CP in the lowest constrained zone (with the heist Margin of Safety) allows more mass reduction there. However, using only the constraint as a criterion to select the refinement points leads to generating all of them near the tip. This is not efficient as the mass is concentrated near the root. This drawback can be avoided by selecting a criterion that combines exploitation (minimum of constraints) and exploration (unsampled zones). In our study, we have proposed a criterion based on two control points.

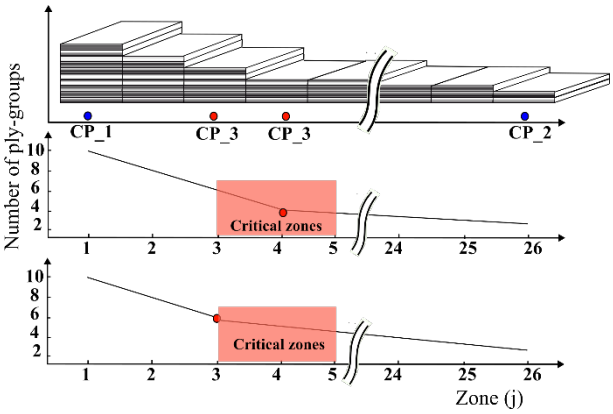

Fig. 11: Effect of adding control points inside or outside the critical region.

Therefore, our demarche starts by identifying the weakest zones characterized by the smallest Margin of Safety (MoS). When a new control point (CP_3) is added inside the critical zones, no improvement in the solution is expected because any change in the author's control points (CP_1 and CP_2) will affect the control point 3 as shown in Fig. 11. However, when the control point (CP_3) is placed at the edge of the critical zones, the first control point (CP_1) can decrease without affecting the control points inside the

critical region. Nevertheless, any decrease in CP_2 will force the critical region control points to decrease, which is not acceptable because this region is already at its limit (theoretically). The critical region is determined by its center and width. The center is simply the zone with the lowest MoS, while the width is a user-defined parameter that can be seen as an additional safety zone. In Fig. 11, the critical region center is zone 4, while its width is 3 zones. In this strategy, two adjacent control points are added at each iteration instead of one, resulting in a complete (from left or right) isolation of the critical region. A complete isolation from both sides (right and left) requires 3 control points.

5.1 Description of optimal solutions

Figures 12, 13, 14, and 15 show the obtained optimal solutions, in terms of objectives, constraints, and deci–sion variables, from the application of the proposed method on the illustrative case study considering the three different refinement strategies. Fig. 12 presents, for each strategy, the convergence history at each refi–nement iteration, the final optimal weight, the constraint values, and a schematic of the inserted control point in each iteration.

The adopted indexation of control points is per–formed as follows. Firstly, the set of CPs of the initial formulation (2 CPs in the present application) is indexed increasingly from the root to the tip (CP_1 and CP_2). Then, during the iterative process, each new CP receives the next index.

In Fig. 12, each curve presents the convergence history for an optimization. Each one corresponds to a formulation with a given set of control points. As shown in Fig. 12, the initial mass for all the optimizations is very close, which is due to the initialization of the GA. Indeed, the initial populations of the GA for the different runs are selected very close to the feasible space. These similar initializations allow a correct com–parison. This figure also shows that the optimization allowed a reduction of about 20 % of the wing mass. In fact, all the strategies stopped at the third iteration (convergence criterion) because the improvement in mass was less than the limit value (e=1%). The conver–gence history shows that the values of the objective function remain invariant for many successive itera–tions, then it jumps to a lower value. This is essentially due to the high number of constraints considered. Indeed, for these generations, the optimizer finds lower masses, but the constraints C1,..5 are not satisfied. Thus, during this number of generations for which the best feasible mass remains constant, the mass wing is reduced considerably. Then, the next best feasible mass is much lower, which explains the jumps in the con–vergence history. This figure also shows that the two constraints, C1 and C2, are activated first. Accordingly, the GA continued reducing the mass until C1 or C2 was activated. According to the results of strategies 1 and 2, the most critical optimization constraint is C2 which is related to the Von Mises failure criterion. In fact, this can be easily justified by the exclusion of the stringers and spar-caps from the design variables. It is also worth mentioning that the C2 value provides valuable insight into the solution's quality, which is very close to the real optimum of this optimization problem. Conversely, the constraints related to the wing tip displacement and torsion C3 and C4 appear to be the least significant ones.

Figures 13, 14, and 15 show the optimal thickness of the different components in terms of the number of plies. This latter is presented directly on the histogram. It shows clearly that the thickness on the tip is reduced drastically compared to the root. All the strategies showed that the optimal thickness of the ribs is the lowest compared with the remaining wing parts, whereas the lower skin is the thickest component. The rib thickness is the lowest, which means that the number of ribs is important in view of the considered constraints. The upper skin thickness is slightly less than the lower one.

5.2 Comparison of Refinement Strategies

Figure 12 allows a better comparison of the three strategies of refinement, which can allow making the following conclusions:

- The selected lowest-complex formulation used only 2 CPs, which is insufficient to get the global opti–mal solutions. However, when increasing the number of control points to four, an important gain in the optimal mass was realized.
- The obtained results clearly confirm that a stra–ightforward formulation is generally very expen–sive. Indeed, 4 CPs are shown to produce the same improvement as 5 CPs and higher. The straight–forward formulation would use 26 CPs.
- The first and the second refinement strategies guarantee a better exploration than the third one but less improvement; this is due to the presence of some control points inside the critical regions, which prevent important mass reduction.
- The refinement criterion has an important effect on the outcomes. Indeed, the third strategy has led to a better improvement when increasing the number of variables. This is because all the inserted CPs ensure the isolation of the critical region from the rest of the zones, offering a chance to reduce mass in the strongest zones.
- A major difference between the third and the other two strategies is that the exploration in the third one is guided by the constraint results from the previous iteration, while it is guided by only the geometry in the first and second strategies.
- Four CPs seem to be sufficient to get an optimal formulation with a significantly reduced cost.

Figure 16 shows a comparison between the optimal solutions in terms of vertical displacement for two strategies with 3 control points. Both the first and second strategies have identical control point locations; hence, only one solution is represented. The solution of the third strategy has a lower mass compared to the other two strategies, which results in a greater displacement, as illustrated in Fig. 16.b.

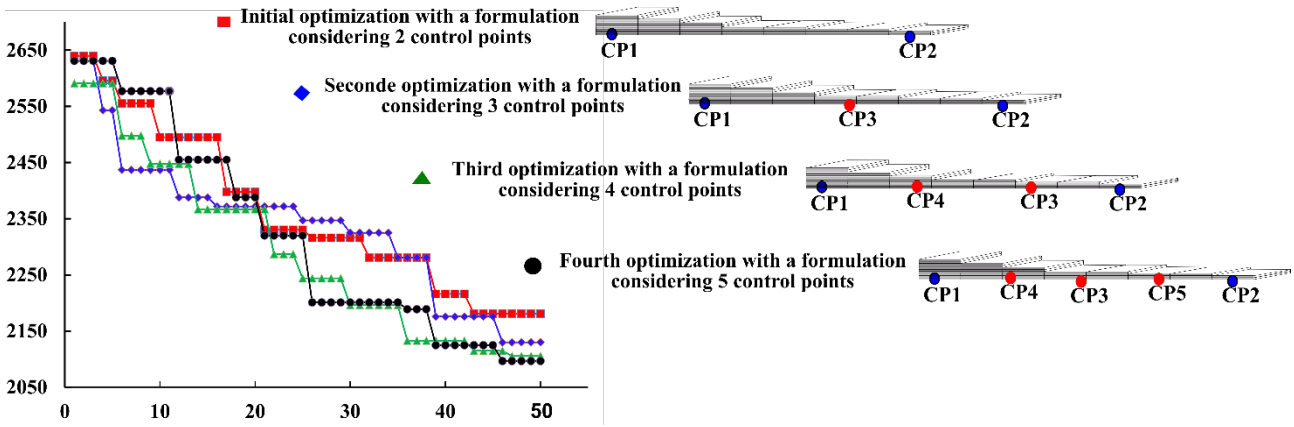

Constraints in the third iteration (5CPs)						Positions of control points (index *j* of zone)				
C1	C2	C3	C4	C5		**CP1**	**CP4**	**CP3**	**CP5**	**CP2**
-0.00791	-0.000245	-0.649	-2.254	0.155		1	7	14	20	26

a) Objectives and constraints of the Strategy 1

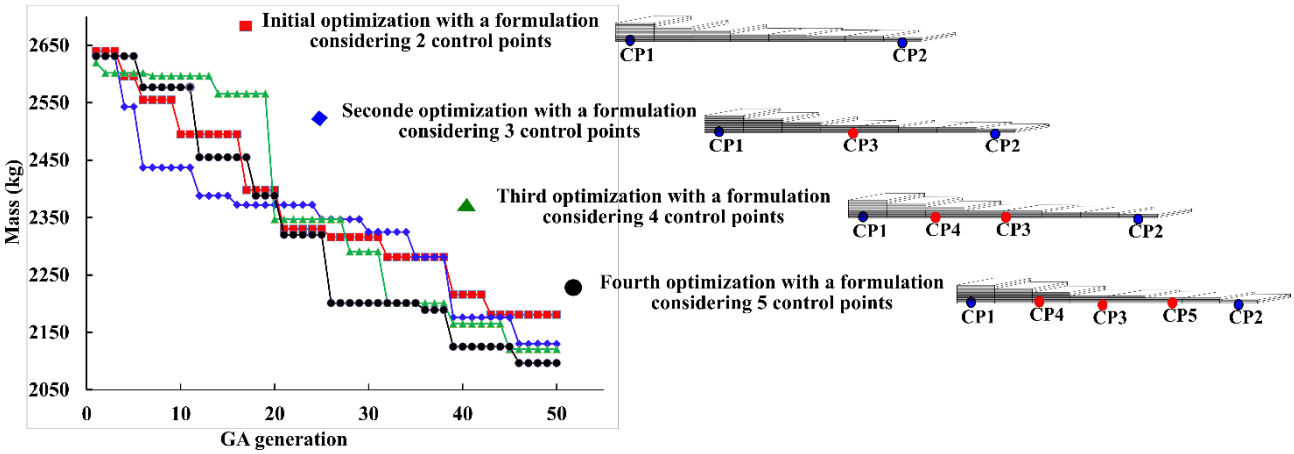

Constraints in the third iteration (5CPs)						Positions of control points (index *j* of zone)				
C1	C2	C3	C4	C5		**CP1**	**CP4**	**CP3**	**CP5**	**CP2**
-0.00791	-0.000245	-0.649	-2.254	-0.155		1	7	14	20	26

b) Objectives and constraints of the Strategy 2

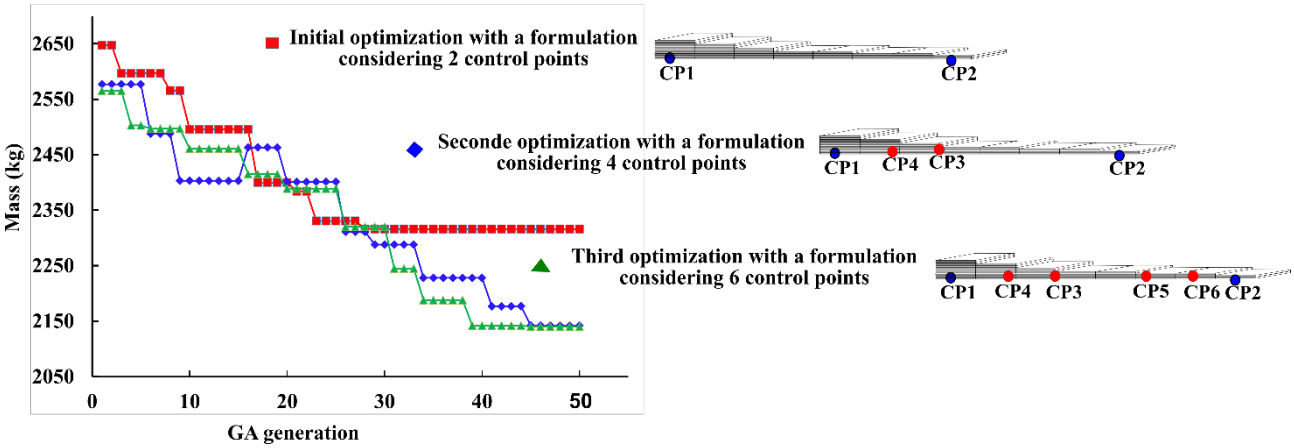

Constraints in the third iteration (5CPs)							Positions of control points (index *j* of zone)				
C1	C2	C3	C4	C5		**CP1**	**CP4**	**CP3**	**CP5**	**CP6**	**CP2**
-0.00371	-0.0001	-0.620	-2.231	-0.153		1	8	9	13	14	26+

c) Objectives and constraints of the Strategy 3

Fig. 12: Optimal solution, in terms of constraints and objectives, of the application of the proposed method on the illustrative case study considering three different refinement strategies

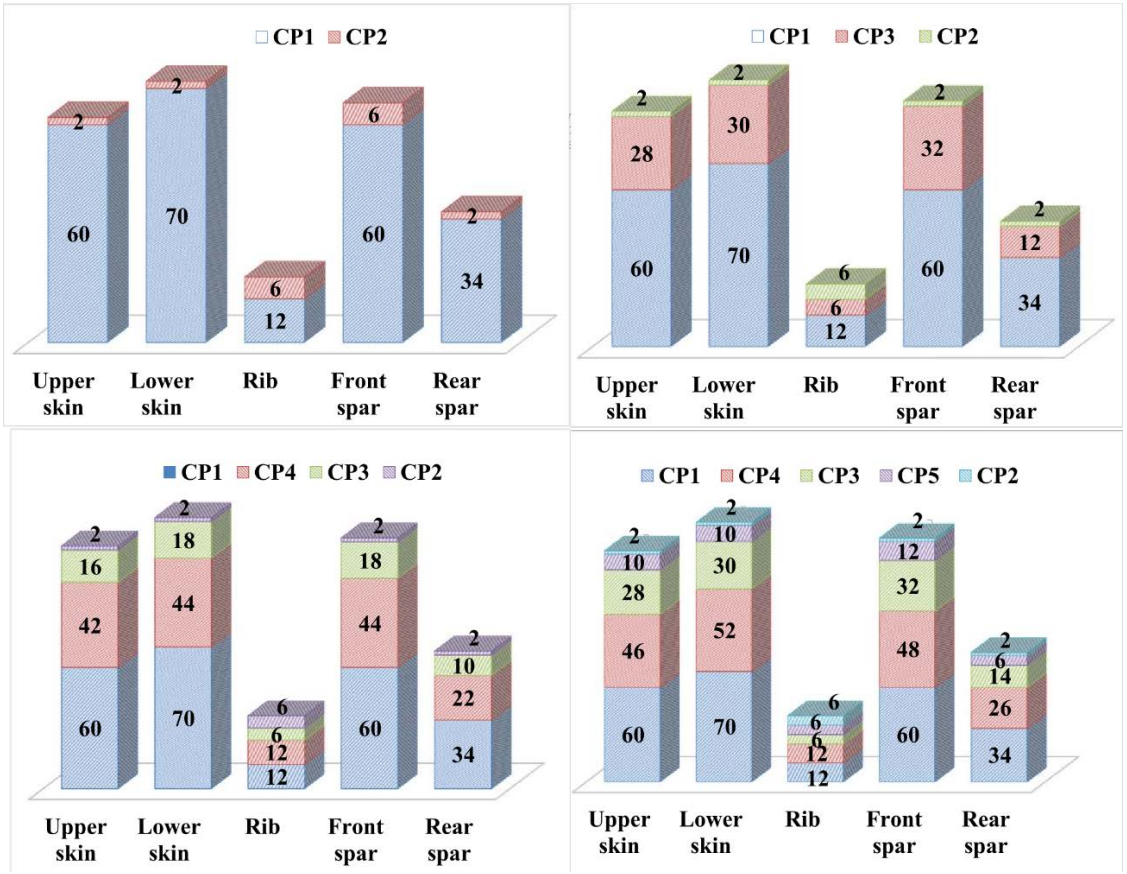

Fig. 13: Optimal solution, in terms of decision variables, of the first strategy.

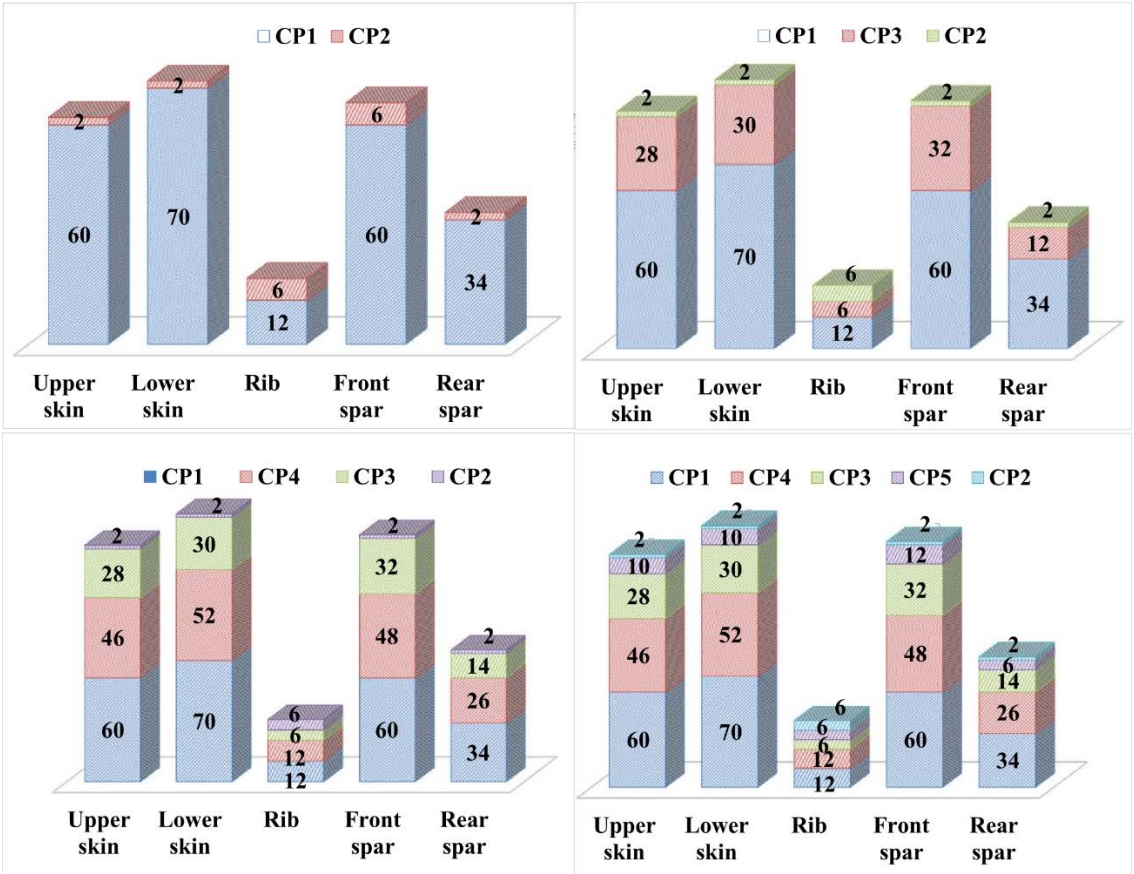

Fig. 14: Optimal solution, in terms of decision variables, of the second strategy.

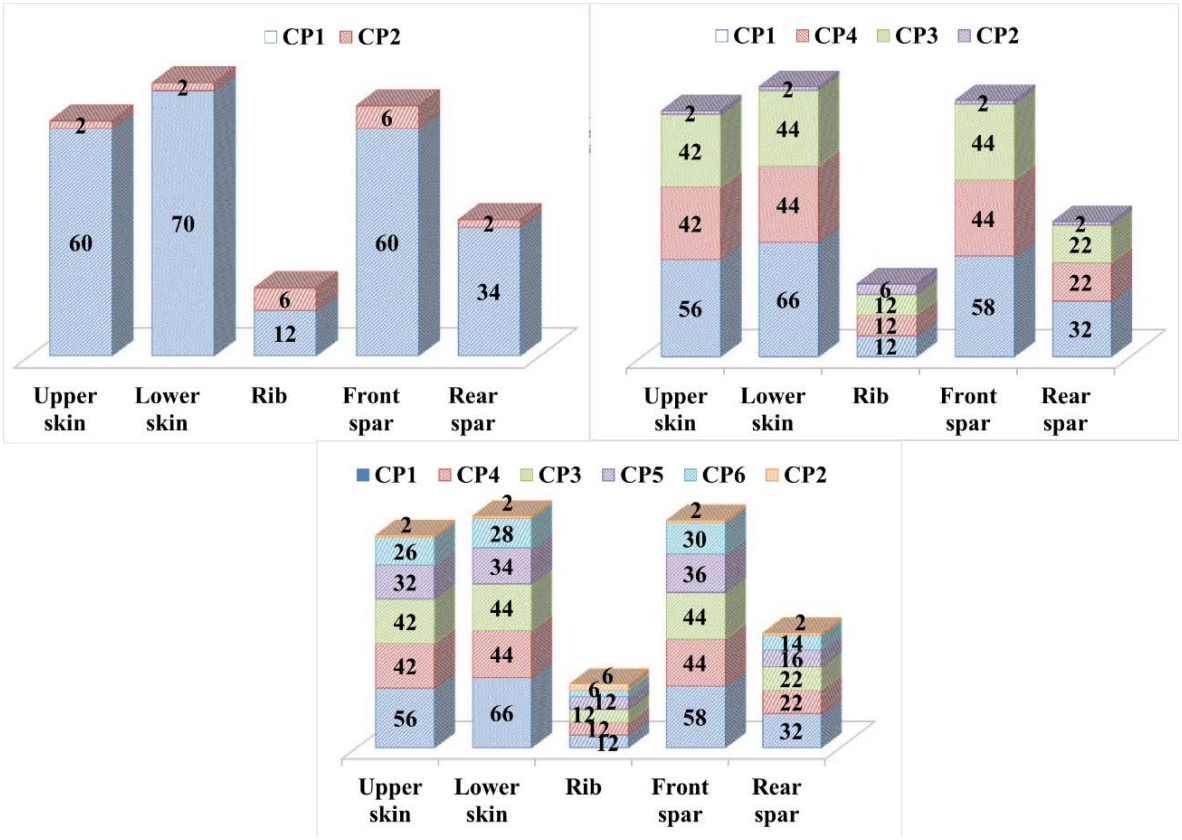

Fig. 15: Optimal solution, in terms of decision variables, of the third strategy.

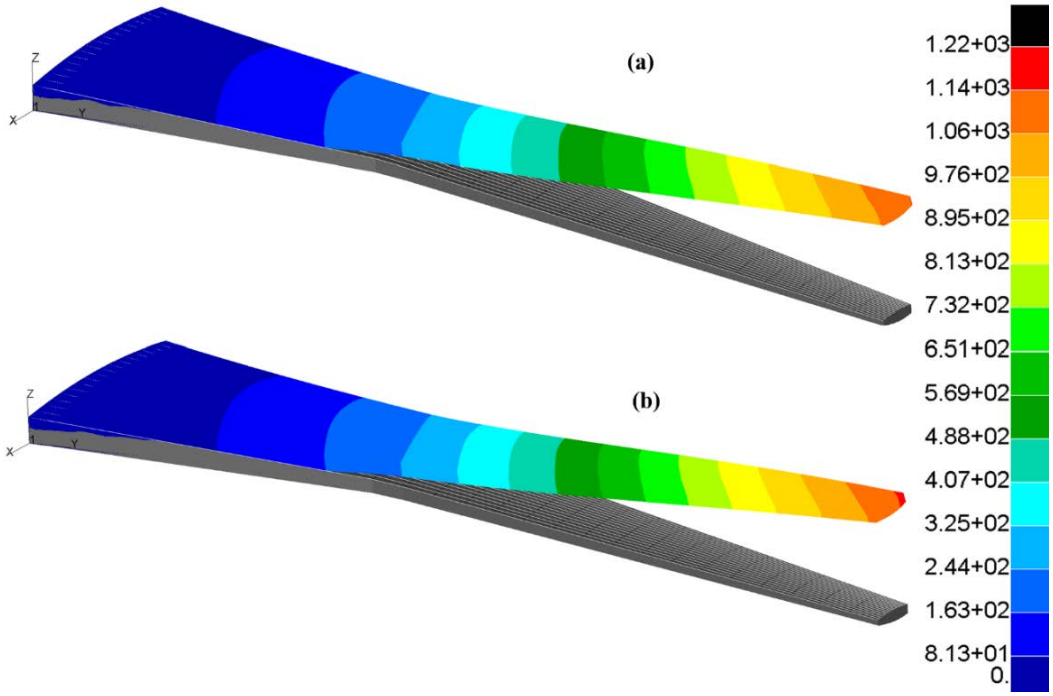

Fig. 16: Vertical displacement results of optimal solutions (in mm) a. Third iteration from strategies 1 and 2 b. Second iteration from strategy 3.

6. CONCLUSIONS

This paper proposes an approach to improve the cost-effectiveness of design optimization of composite structures. It aims to adjust the formulation complexity and reduce the solving cost. This approach is based on a descendant ascendant scheme, which decreases the formulation complexity to its lowest level and then increases it using an adaptive process. The latter adds variables until reaching the right-complex formulation. This idea is validated by the design of a composite material wing box from the literature. Therefore, an implementation was performed, coupling a FEM solver with a GA optimizer. A multi-scale solver is proposed here to reduce the cost of optimization further. A straightforward application of this formulation leads to 26 zones; each one encapsulates 5 variables. The application of the proposed approach reduces this

formulation to the lowest level (2 zones), then increases it adaptively until 5 zones.

Many conclusions arise from this application; namely, it revealed that the straightforward formulation is very expensive. Indeed, the same results were obtained for 26 zones with just 5 zones. This approach involves many techniques, such as the determination of the lowest-complex formulation and the refinement process, which require careful tuning. The adaptive refinement uses a criterion to select additional variables. This criterion has an important effect on the outcomes of the approach. Particularly, criteria with weak exploration potential lead to an expensive refinement.

Theoretically, the proposed V-approach can be considered a general-purpose paradigm, which can be applied to different optimization problems that involve a complex formulation. In this case, the V-approach can predict the right complex problem. Indeed, after the initial formulation, the process of this method handles variables independently of their types. One advantage of this method is its ease of application since it is based on the initial formulation, which must be established by the user before applying it. For instance, the wing-box application revealed an easy applicability of this approach. This is mainly due to the type of initial formulation. The second advantage is that it can use some existing criteria to ensure the maximum exploration of the lowest complex formulation and the exploration-exploitation of the refinement process. However, for particular problems, users of this method should consider the particularity manually. For instance, if the problem contains a variable that is important for the functionality of the optimized system, it must be maintained in the lowest complex formulation. In this context, this applicability can be improved via more tests, which can be the object of upgraded versions of this method.

Many ideas can be added and tested to improve this approach. For instance, a criterion to select the newly added control point can be elaborated using statistical methods. Indeed, a good selection of new control points can reduce further the complexity of the problem. Moreover, the constructed lowest-complex formulation may influence the complexity and the solution of the final problem. Therefore, an investigation of this method and its impact on the process may further improve the applicability of the present strategy.

REFERENCES

[1] Garinis D., Dinulovic M, Rašuo B.: Dynamic Analysis of Modified Composite Helicopter Blade, FME Transactions, Vol. 40 No 2, 2012, pp 63-68.

[2] M.D. Milenković-Babić, D.A. Ivković, B.G. Osto–jić, B.Z. Dovatov, M.S. Trifković, V.D. Antonić, Flying Wing Conceptual Design and Flight Testing, FME Transactions, Vol. 52 No 4, 2024.

[3] G. Moors, C. Kassapoglou, de S.F.M. Almeida, C.A.E. Ferreira, Weight trades in the design of a composite wing box: effect of various design choices. CEAS Aeronaut J 10, 403–417 (2019). https://doi.org/10.1007/s13272-018-0321-4

[4] M. Esposito, M. Gherlone, Composite wing box deformed-shape reconstruction based on measured strains: Optimization and comparison of existing approaches, Aerospace Science and Technology, Volume 99, 2020, 105758, https://doi.org/10.1016/j.ast.2020.105758.

[5] Mirko Dinulović, Boško Rašuo, Ana Slavković, Goran Zajić, Flutter Analysis of Tapered Composite Fins: Analysis and Experiment, FME Transactions, Vol. 50 No 3, 2022.

[6] Azhar K. Farhood, Ahmed A. Ali, THE STATIC ANALYSIS OF COMPOSITE AIRCRAFT WING-BOX STRUCTURE, Journal of Engineering, 2011, Volume 17, Issue 6, Pages 1378-1390.

[7] C. You, M. Yasaee, S. He a, D. Yang, Y. Xu, I. Dayyani, H. Ghasemnejad, S. Guo, P. Webb, J. Jennings, G. Federico, Identification of the key design inputs for the FEM-based preliminary sizing and mass estimation of a civil aircraft wing box structure, Aerospace Science and Technology, Volume 121, 2022, 107284

[8] Ys. Meng, L. Yan, W. Huang, Structural design and analysis of a composite wing with high aspect ratio. J. Zhejiang Univ. Sci. A 20, 781–793 (2019). https://doi.org/10.1631/jzus.A1900271

[9] Stamatelos, D., Labeas, G. Towards the Design of a Multispar Composite Wing. *Computation* 2020, *8*, 24. https://doi.org/10.3390/computation8020024.

[10] Stamatelos, D.; Labeas, G. (2011). Investigation on a multispar composite wing. Proceedings of the Institution of Mechanical Engineers Part G Journal of Aerospace Engineering. 226. 88. 10.1177/0954410011406476.

[11] Dähne, S., Hühne, C. (2018). Gradient Based Structural Optimization of a Stringer Stiffened Composite Wing Box with Variable Stringer Orientation. Advances in Structural and Multidisciplinary Optimization. WCSMO 2017. Springer, Cham. https://doi.org/10.1007/978-3-319-67988-4_62.

[12] Farsadi T, Bozkurt MO, Coker D, Kayran A. Improvement of structural characteristics of composite thin-walled beams using variable stiffness concept via curvilinear fiber placement. Proceedings of the Institution of Mechanical Engineers, Part G: Journal of Aerospace Engineering.2021; 235(14):2017-2032. doi:10.1177/0954410020988240

[13] Francesco Toffol, Sergio Ricci, A Meta-Model for composite wingbox sizing in aircraft conceptual design, Composite Structures, Volume 306, 2023, https://doi.org/10.1016/j.compstruct.2022.116557.

[14] V. Cipolla, K. Abu Salem, G. Palaia, V. Binante, D. Zanetti, A DoE-based approach for the implemen–tation of structural surrogate models in the early stage design of box-wing aircraft, Aerospace Science and Technology 117 (2021)

[15] S.B. Mulani, V. Duggirala, R.K. Kapania, Curvi–linearly T-stiff-ened panel-optimization framework

under multiple load cases using parallel processing. J. Aircr. 50, 1540–1554 (2013)

[16] Q. Liu, M. Jrad, S.B. Mulani, R.K. Kapania, Global/local optimization of aircraft wing using parallel processing. AIAA J. 54, 1–11 (2016)

[17] Liu, B., Haftka, R. & Akgün, M. Two-level composite wing structural optimization using response surfaces. Struct Multidisc Optim 20, 87–96 (2000). https://doi.org/10.1007/s001580050140.

[18] Guo S, Li D, Liu Y. Multi-objective optimization of a composite wing subject to strength and aeroelastic constraints. Proceedings of the Institution of Mechanical Engineers, Part G: Journal of Aerospace Engineering. 2012; 226(9): 1095-1106. doi:10.1177/0954410011417789

[19] Wang, Y., Ouyang, X., Yin, H., Yu, X. (2015). Structural-Optimization Strategy for Composite Wing Based on Equivalent Finite Element Model. Journal of Aircraft. 53. 1-9. 10.2514/1.C033469.

[20] Fischer M, Kennedy D, Featherston CA. Multilevel framework for optimization of lightweight structures. Proceedings of the Institution of Mechanical Engineers, Part G: Journal of Aerospace Engineering. 2012; 226(4):380-394. doi:10.1177/0954410011411637

[21] Carrera E, Mannella L, Augello G, Gualtieri N. A two-level optimization feature for the design of aerospace structures. Proceedings of the Institution of Mechanical Engineers, Part G: Journal of Aerospace Engineering. 2003; 217(4):189-206. doi:10.1243/095441003769700753

[22] Q. Zhao, Y. Ding, H. Jin, A Layout Optimization Method of Composite Wing Structures Based on Carrying Efficiency Criterion, Chinese Journal of Aeronautics, Volume 24, Issue 4, 2011, Pages 425-433, ISSN 1000-9361, https://doi.org/10.1016/S1000-9361(11)60050-2.

[23] Dababneh, O.; Kipouros, T.; Whidborne, J.F. Application of an Efficient Gradient-Based Optimiz<–ation Strategy for Aircraft Wing Structures. *Aerospace* 2018, *5*, 3. https://doi.org/ 10.3390/aerospace5010003.

[24] Rongrong, X. & Zhengyin, Y. & Kun, Y. & Gang, W. (2018). Composite material structure optimization design and aeroelastic analysis on forward swept wing. Proceedings of the Institution of Mecha–nical Engineers, Part G: Journal of Aerospace Engineering. 233. 095441001880781. 10.1177/0954410018807810.

[25] [S. Kilimtzidis, A. Kotzakolios, V. Kostopoulos, Efficient structural optimization of composite materials aircraft wings, Composite Structures, Volume 303, 2023, 116268, ISSN 0263-8223, https://doi.org/10.1016/j.compstruct.2022.116268.

[26] Elyasi, M., Roudbari, A. & Hajipourzadeh, P. Multi-objective robust design optimization (MORDO) of an aeroelastic high-aspect-ratio wing. *J Braz. Soc. Mech. Sci. Eng.* **42**, 560 (2020). https://doi.org/10.1007/s40430-020-02633-7

[27] Farrokh, M., Fallah, M.R. Flutter instability boundary determination of composite wings using adaptive support vector machines and optimization. *J Braz. Soc. Mech. Sci. Eng.* **45**, 181 (2023). https://doi.org/10.1007/s40430-023-04098-w

[28] P. Jin, B. Song, X. Zhong, Structure optimization of large composite wing box with parallel genetic algorithm, J. Aircr. 48 (6) (2011) 2145–2148, http://dx.doi.org/10.2514/1.C031493.

[29] Yin Hailian, Yu Xiongqing, Integration of Manufacturing Cost into Structural Optimization of Composite Wings, Chinese Journal of Aeronautics, Volume 23, Issue 6, 2010, Pages 670-676, ISSN 1000-9361, https://doi.org/10.1016/ S1000-9361(09)60269-7.

[30] Panettieri, E., Montemurro, M., Fanteria, D. et al. Multi-scale Least-Weight Design of a Wing-Box Through a Global/Local Modelling Approach. J Optim Theory Appl 187, 776–799 (2020). https://doi.org/10.1007/s10957-020-01693-y.

[31] Benaouali A., S. Kachel, Multidisciplinary design optimization of aircraft wing using commercial software integration, Aerospace Science and Technology, Volume 92, 2019, Pages 766-776, ISSN 1270-9638, https://doi.org/10.1016/j.ast. 2019.06. 040.

[32] [Soutis, C., Fibre reinforced composites in aircraft construction, Progress in Aerospace Sciences, Volume 41, Issue 2:143-151, 2005.

[33] Chand, S. Review Carbon fibers for composites. Journal of Materials Science 35, 1303–1313 (2000). https://doi.org/10.1023/A:1004780301489

[34] Evans, E.E., Brooks, R.A., Liu, J. et al. Comparison of X-ray Computed Tomography and Ultrasonic C-Scan Techniques and Numerical Modelling of Impact Damage in a CFRP Composite Laminate. Appl Compos Mater 31, 249–264 (2024). https://doi.org/10.1007/s10443-023-10171-3.

[35] J. Svorcan, Z. Trivković, T. Ivanov, M. Baltić, O. Peković, Multi-objective Constrained Optimizations of VAWT Composite Blades Based on FEM and PSO, FME Transactions, Vol. 52 No 4, 2024.

[36] S. Boria, J. Obradovic, G. Belingardi, Giovanni. (2017). On Design Optimization of a Composite Impact Attenuator under Dynamic Axial Crushing. FME Transaction. 45. 435-440.

[37] O. Seresta, Z. Gurdal, D. B. Adams, L. T. Watson, Optimal design of composite wing structures with blended laminates, Composites Part B: Engineering, Volume 38, Issue 4, pp 469-480, 2007, doi.org/10.1016/j.compositesb.2006.08.005.

[38] H. Zhang, X. Zheng, Z. Liu, Optimization Of Composite Wing Using Genetic Algorithm, 21st International Conference on Composite Materials Xi'an, 20-25th August 2017.

[39] S. Kilimtzidis, A. Kotzakolios, V. Kostopoulos, An Efficient Optimization Scheme For The Preliminary Sizing Of Composite Aircraft Wings, International Forum on Aeroelasticity and Structural Dynamics, IFASD 2022, 13-17 June 2022, Madrid, Spain.

[40] P.W. Aung, O. Tatarnikov, N. L.Aung, Structural optimization of a light aircraft composite wing, IOP Conf. Series: Materials Science and Engineering 709 (2020) 044094, doi:10.1088/1757-899X/709/4/044094.

[41] S. Khalfallah, H. Lehtihet, "A multi-objective optimization methodology based on multi-mid-range meta-models for multimodal deterministic/ robust problems," Structural and Multidisciplinary Optimization, vol. 60, no. 6, pp. 2373–2389, 2019.

[42] S. Shrivastava, P.M. Mohite, Design and Optimization of a Composite Canard Control Surface of an Advanced Fighter Aircraft under Static Loading, Curved and Layered Structures, 2(1), 2015, DOI:10.1515/cls-2015-0006.

[43] P. Jin, B. F. Song, X. P. Zhong, Structure optimization of large composite wing with parallel genetic algorithm, Jornal of Aircraft. 48 (2011) 2145-2148

[44] X.P. Zhong, P. Jin, Q. Han, A Method for Composite Wing Box Optimization with Manufacturing Constraints, International Conference on Power Electronics and Energy Engineering, 2015, DOI: 10.2991/peee-15.2015.61.

[45] McMahon MT, Watson LT., A distributed genetic algorithm with migration for the design of composite laminate structures. Parallel Algorithms Appl 2000; 14:329–62

NOMENCLATURE:

ANOVA	Analysis of Variance
C1, C2, C3, C4, C5	Optimization constraints
CP	Control Point
d_{tip}	vertical displacement at the wing tip
e	Target precision
E	Young's modulus
FEA	Finite element Analysis
FEM	Finite element method
fobj	Objective function
G	Shear modulus
GA	Genetic Algorithm
GFEM	Global Finite element method
LFEM	Local Finite element method
mbr	Structural member of the wing-box
N	Number of control points
Np	Number of ply-group
P	GA Population size
X	Vector of decision variables
Solp	Optimal mass before adding a CP
Solc	Optimal mass after adding a CP
X^t, X^c, Y^t, Y^c	Allowable stresses of the ply
y	Spanwise coordinate
Wi	Mass of the structural element i
σ_x, σy, and τ_{xy}	The ply stresses expressed in the ply coordinate system
σ_{VM}	The Von Mises equivalent stress,
σ_{allow}	Allowable stress of the isotropic material
ε	Relative difference between previous and current optimal solutions
θ_{tip}	torsional twist at the wing tip
ν	Poisson's ratio
ρ	Density

СТРАТЕГИЈА ОПТИМИЗАЦИЈЕ ДИЗАЈНА КОМПОЗИТНЕ КУТИЈЕ КРИЛА АВИОНА ЗАСНОВАНА НА ВИШЕРАЗМЕРНОМ ФЕА

С. Фарах, С. Калфалах, А. Бутемеђет, Л. Реби

Оптимизација дизајна композитних крила је сложен проблем који укључује бројне параметре материјала и облика. Овај рад предлаже две идеје за ефикасно решавање таквог проблема, а то су десна-комплексна формулација проблема оптимизације и коришћење анализе коначних елемената на више скале (ФЕА). Прва идеја се постиже по В шеми (десцендентна асцендентна шема). У силаску, сложеност проблема се своди на најнижи ниво (најниже сложене формулације), што можда неће бити довољно за добијање потенцијалних решења. Сходно томе, врши се адаптивни процес, прогресивно повећавајући сложеност додавањем нових варијабли док се не постигне формулација десног комплекса. ФЕА на више нивоа комбинује глобалну и локалну анализу методе коначних елемената (ФЕМ). Глобални анализира статичност глобалног домена, што открива најкритичнији панел. Овај последњи анализира феномен извијања локално и прецизније. Ова стратегија је потврђена оптимизацијом композитне кутије крила из литературе и узимањем у обзир добро познате формулације засноване на зонама. Према томе, формула најниже сложености је дефинисана са минималним могућим бројем зона крила, а затим се прилагођава итеративним повећањем броја крилних зона. Овај процес се зауставља када оптимално решење постане непроменљиво. Ова апликација настоји да минимизира масу крила под многим ограничењима, као што је максимални Von Mises напон. Проблем је решен спајањем оптимизатора генетског алгоритма (ГА) са вишеразмерним ФЕА. Резултати су показали да је усвојена стратегија детектовала формулацију десног комплекса, што је значајно повећало време израчунавања уз значајно повећање масе крила у односу на критеријум отпорности.